Atmospheric Oxidation of Methyl Propanoate by the OH radical

Mohamed A. M. Mahmoud,[1] Safinaz H. El-Demerdash [1] Tarek M.El-Gogary,[2,3,*] Ahmed M. El-Nahas[1,*]

[1]Chemistry Department, Faculty of Science, Menoufia University, 32512 Shebin El-kom, Egypt.

[2]Chemistry Department, Faculty of Science, Jazan University, 2097 Jazan, KSA.

[3]Chemistry Department, Faculty of Science, Damietta University, 34517 New Damietta, Egypt

Abstract

Atmospheric oxidation of methyl propanoate (**MP**) by the OH radical has been performed using density functional theory (BMK, BBIK) and ab initio (MP2, CBS-QB3) calculations. The thermodynamic and kinetic parameters are calculated. Three channels have been discussed. These reactions occur through low energy barriers of 3.2–4.3 kcal/mol. The energy barriers increase in the order $\alpha < \mu < \beta$ at CBS–QB3. However, BMK shows slightly different order. Rate constants and branching ratios reveal that the H-abstraction from C_α is as the dominant reaction over the whole temperature range of 200–300 K, with a competition from C_β channel at lower temperature. The BB1K data reproduce the available experimental rate constant.

Keywords: Methyl propanoate, atmospheric oxidation, DFT, ab initio, rate constants.

*Corresponding authors. E-mail: amelnahas@hotmail.com (Ahmed El-Nahas), tarekelgogary@yahoo.com (Tarek El-Gogary)

1. Introduction

The growing use of fossil fuels raises large concerns about energy security, emission of pollutants, and climate change. Therefore, search for fuel alternatives becomes a must. Biodiesel consists mainly of methyl esters, and can be produced from renewable energy sources, such as animal fats, vegetable oils, algae and waste oils [1]. There have been a few studies [2-4] on reaction kinetics of large esters because of their low vapor pressure and chemical complexity. Short-chain fatty acid methyl esters (FAMEs) possess the ester structure but lack the long-chain alkane structure [5].

Alkyl esters [6-9], oxygenated volatile organic compounds, are emitted directly to the atmosphere from both natural and anthropogenic sources [6-9]. Natural sources of esters include emissions from vegetation and fruit. Anthropogenic emissions of the unsaturated esters to the atmosphere can occur during their production, processing, storage and disposal [6-9].

The widespread use of fatty acid alkyl esters in diesel blends will lead to their release into the atmosphere. Atmospheric degradation of methyl propanoate (**MP)**, a model for larger esters present in biodiesel**,** is initiated by photochemical oxidants such as the hydroxyl radical, which is present at a concentration of approximately 1×10^6 radicals cm^{-3} [10]. Detailed kinetic and mechanistic data concerning these reactions are needed as inputs for atmospheric chemistry models to assess the environmental impacts associated with release of esters into the air. The available database regarding the atmospheric chemistry of esters is limited [11, 12] and the current work was undertaken to improve our understanding of the chemistry of this class of oxygenated compounds**.**

Some experimental and theoretical [5, 6, 9-16] studies of small alkyl esters have been reported. Computational chemistry has become an important source of knowledge of specific reaction rates and mechanisms [17, 18].

As regards to short-chain FAMEs, **MP** represents the smallest methyl ester containing CC bond alpha to the carbonyl group. Besides, **MP** is an intermediate product with comparatively high concentrations in the decomposition of biodiesel such as the rapeseed methyl ester (RME) [19].

In the present work, we study thermochemistry and kinetics of oxidation of **MP** by the atmospheric OH radical in continuation of our previous work on the uni-

and bimolecular decomposition of different volatile oxygenated compound especially biofuels [20-28], to understand its fate in the atmosphere.

This paper is organized as follows: Section 2 gives details of the computational methods. Section 3 presents the results and discussion and is divided into four subsections. This is followed by Section 4, which summarizes main conclusions.

2. Computational details

The reactants, intermediates, products and different transition states were fully optimized with the density functional theory of Boese and Martin (BMK) [29] in conjunction with the 6-31+G(d,p) basis set. Vibrational frequency calculations have been conducted for each stationary point at the same level to characterize its nature as minimum or transition state on the potential energy surface (PES) of the relevant system. Transition states have only one imaginary frequency (first order saddle points) while minima show real frequencies. The frequencies are scaled with 0.95[30]. Minimum energy paths (MEP) were carried out at BMK through intrinsic reaction coordinate (IRC) [31, 33] scheme to verify that each transition state connects the reactants with the desired products. Energies were refined at BMK, Becke88 Becke95 1-parameter model for kinetics (BB1K) [34, 35] and second-order Møller–Plesset perturbation theory (MP2) [36] using 6-311++G(2d,2p) basis sets. For simplicity, energies at higher levels will be referred to as BMK, BB1K and MP2, respectively. Single point multi-level CBS-QB3 [37-41] calculations have also been done to get more accurate energies.

All calculations were performed using the Gaussian-16W package [42]. Molecular structures were visualized and manipulated with the Chemcraft program V1.8 [43]. Based on the good performance of the high-level CBS-QB3 calculations when compared with experiment, the BB1K energetics were found to be superior to BMK [44]. The thermodynamic expression of the equilibrium constant (K_{eq}) [28] for gas-phase reactions is:

$$K_{eq} = \exp \Delta G^{0}(T)/RT \qquad (1)$$

where ΔG^{0} is standard reaction Gibbs free energy at temperature T, R is the universal gas constant.

Rate constants (k) for the bimolecular decomposition of **MP** are calculated using conventional transition state theory (TST) as equation (2) [45-49] including one-dimensional (1D) tunneling effects Wigner (W) [50, 51].

$$k_{TST} = \frac{k_B T}{h} \frac{Q_{TS}}{Q_{MP}\, Q_{OH}} exp\left(-\frac{E_0^{\#}}{R\, T}\right) \qquad (2)$$

In the above equation [50, 51], Q_{MP}, Q_{OH} and Q_{TS} represent the total molecular partition functions for the reactants, and transition state, $E_0^{\#}$ is the zero-point energy corrected energy barrier, k_B, h, T and R represent the Boltzmann's and Planck's constants, temperature, and the universal gas constant respectively. We have also included the transmission coefficient $\chi(T)$ to account for the tunneling effect along the reaction coordinate and, thus, the rate constant $k_{TST/W}(T)$ including tunneling correction is given by

$$k_{TST/W}(T) = \chi(T)\, k_{TST}(T) \qquad (3)$$

The transmission coefficient $\chi(T)$ was calculated using the Wigner correction [50, 51], which is the simplest form and assumes a parabolic potential for the nuclear motion near the transition state. The Wigner transmission coefficient is given by

$$\chi(T) = 1 + 1/24\, [h\nu/k_B\, T]^2 \qquad (4)$$

where ν is the imaginary frequency in the transition state.

TST gives an estimate of the rate constants as a function of the temperature, and is known to give reliable estimations of rate constants [52, 53]. K_{eq} and k calculations were performed using the kinetic and statistical thermodynamical package (KiSThelP) 2016-v1of Canneaux et al [54].

3. Results and discussion

Reaction of $^{\bullet}OH$ with **MP** occurs through H-abstraction from different position of carbon atoms, C_α, C_β, and C_μ with formation of various radicals and water. The reactions (R1-3) pass through pre- and post-reaction intermediates. These oxidation reactions (R1-3) are illustrated in Scheme 1 and summarized as follows:

R1, $CH_3CH_2C(O)OCH_3 + {}^{\bullet}OH \rightarrow CH_3C^{\bullet}HC(O)OCH_3 + H_2O$

R2, $CH_3CH_2C(O)OCH_3 + {}^{\bullet}OH \rightarrow CH_3CHC(O)OC^{\bullet}H_2 + H_2O$

R3, $CH_3CH_2C(O)OCH_3 + {}^{\bullet}OH \rightarrow C^{\bullet}H_2CH_2C(O)OCH_3 + H_2O$

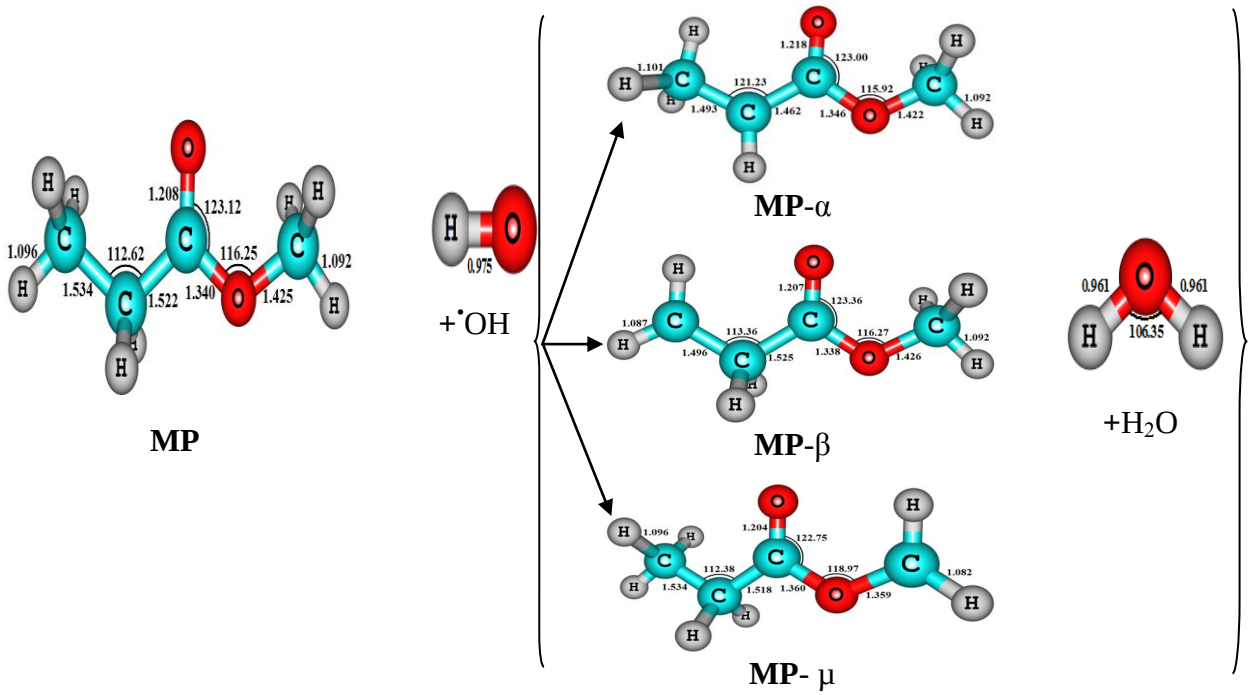

Scheme 1 H-abstraction reactions from **MP** by •OH, resulting in three reaction channels.

3.1. Structures

Structures and energetics of reactants, transition states, intermediates and products are presented in the following-subsections. Figs. 1 and 2 display the optimized structures of the most stable form of **MP** along with three transition states for its oxidation by the •OH radical. The calculated equilibrium bond length of the hydroxyl radical of 0.975 Å is in a good accord with the experimental distance of 0.970 Å [55].

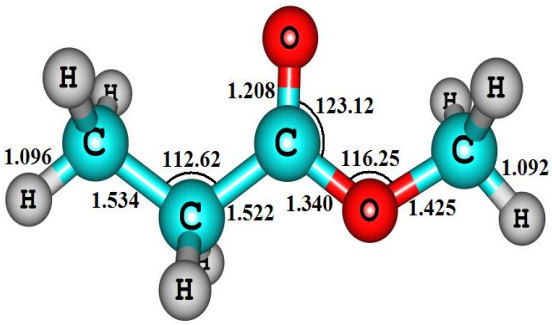

Fig. 1. Optimized structures of **MP** at BMK/6-31+G(d,p). Bond lengths are given in Ångstroms and angles in degrees.

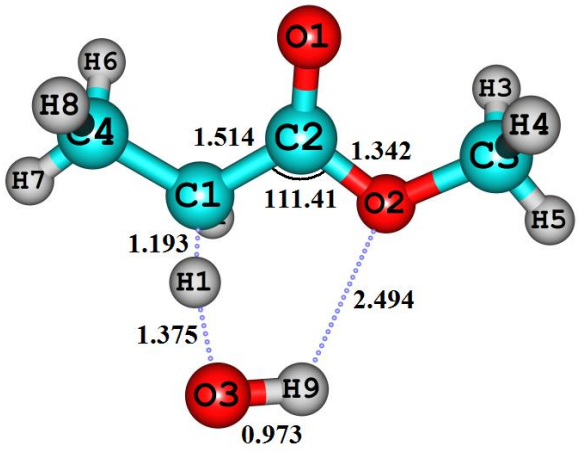

TS-α

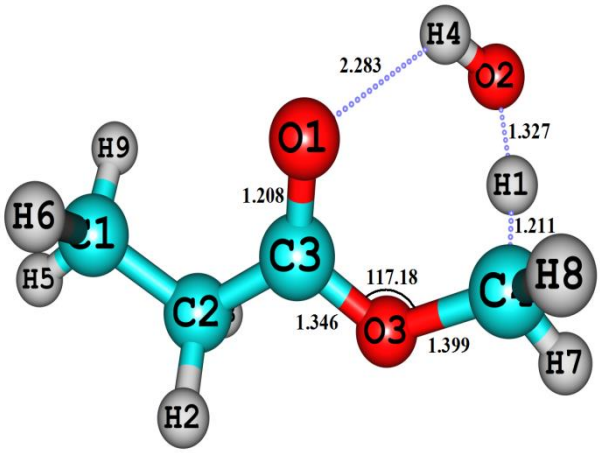

TS-μ

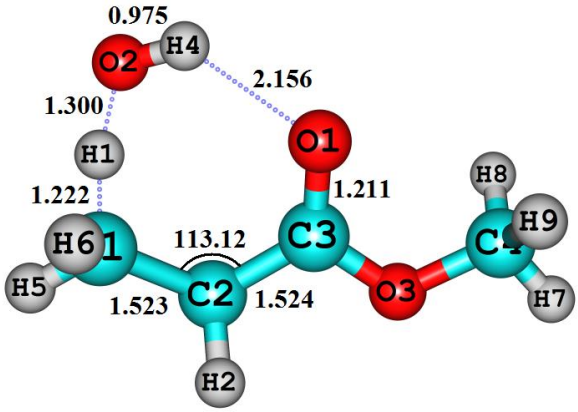

TS-β

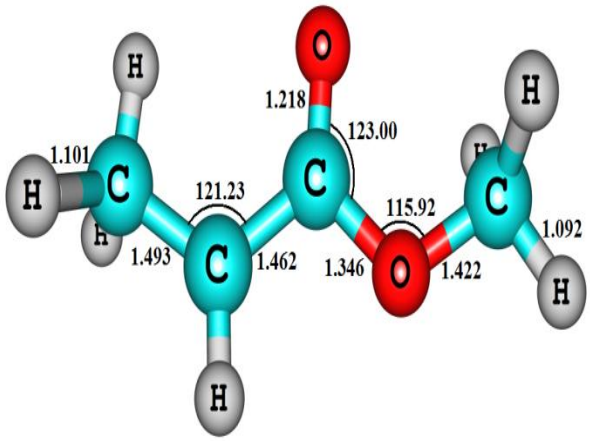

MP-α, $CH_3C^{\bullet}HC(O)OCH_3$

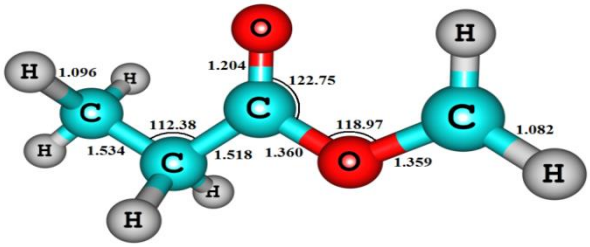

MP- μ, $CH_3CHC(O)OC^{\bullet}H_2$

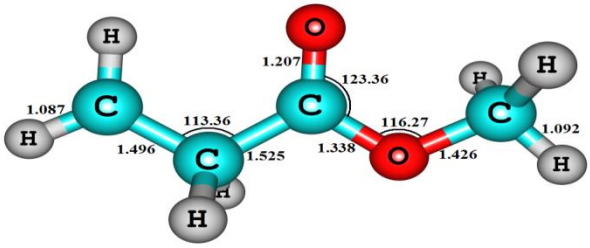

MP-β, $C^{\bullet}H_2CH_2C(O)OCH_2$

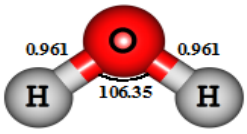

H_2O

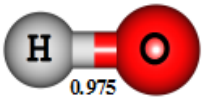

$^{\bullet}OH$

Fig. 2. Optimized structures of transition states (TSs), products, pre-complexes and post-complexes for H-abstraction from **MP** by $^{\bullet}OH$ at BMK/6-31+G(d,p). Bond lengths are given in Ångstroms and angles in degrees.

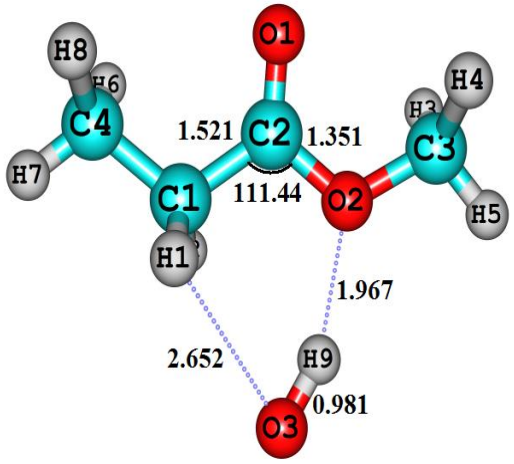

MP-α pre-complex

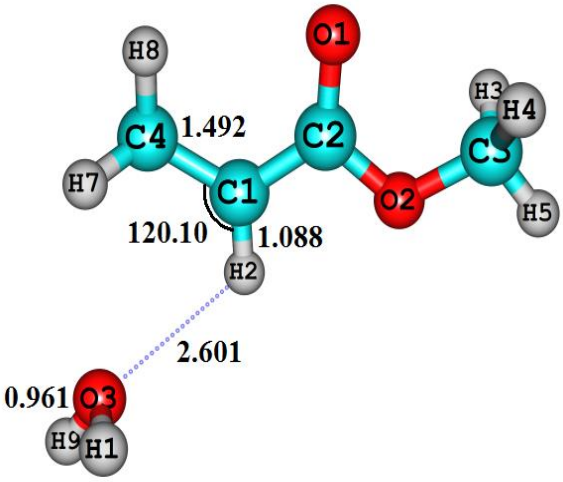

MP-α post-complex

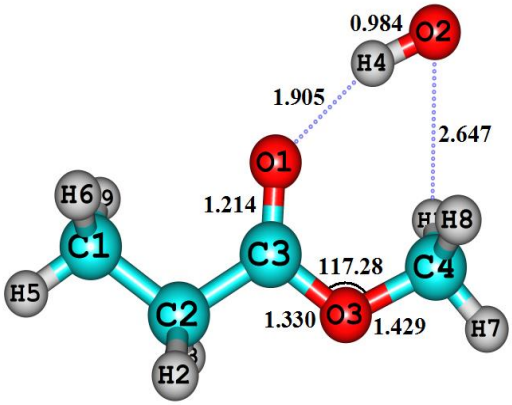

MP-μ pre-complex

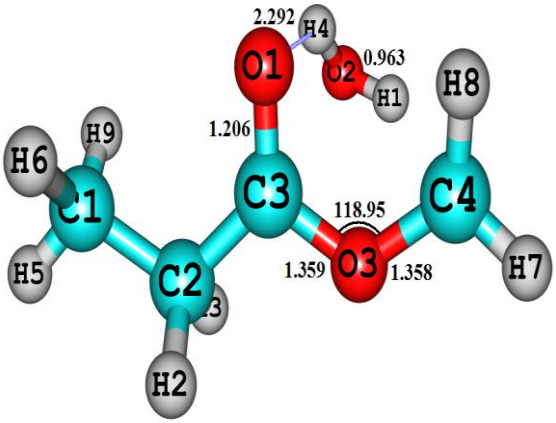

MP-μ post-complex

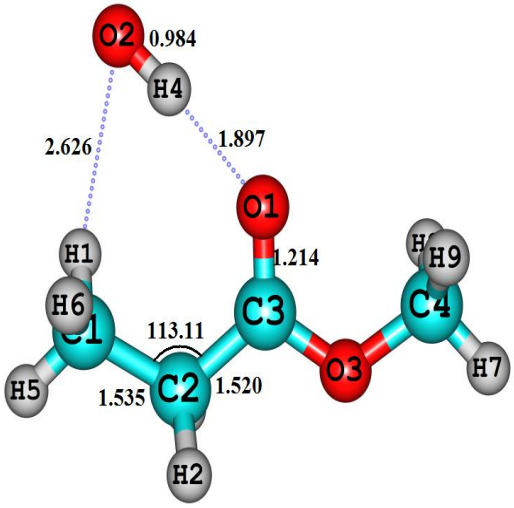

MP-β pre-complex

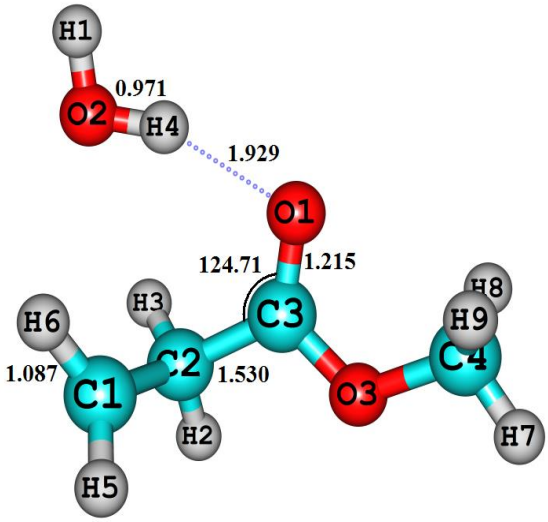

MP-β post-complex

Fig. 2. Continuous

Three transition states have been located in the course of such H-abstraction reactions. The pre-reactive intermediates represent hydrogen bonded complexes with hydrogen bond lengths of 2.156–2.494 Å. Pre-reactive complexes exist between reactants and transition states, while post-reactive complexes are located between transition states and products. The breaking/forming bonds for R1, R2, and R3 are elongated by 8.13/30.1, 9.6/27.6 and 10.3/26.1%, respectively. This agrees with the Hammond postulate [56] for exothermic reactions which addresses closeness of the structure and energy of the transition state to the reactants rather than the products. The resemblance between the structures and energies of a transition state and reactant increases with increasing of exothermicity of the reaction [56].

3. 2. Energetics

A plot of potential energy diagram using BMK, BB1K and CBS-QB3 levels of theory for the oxidation of **MP** with $^{\bullet}$OH is illustrated in Fig. 3. Energy profiles for all possible pathways from IRC calculations are displayed in the supporting information. An inspection of Fig. 3 indicates that, H-abstraction from C_α is the most thermodynamically and kinetically favored reaction on the potential energy surface (PES) of the complex decomposition of **MP**. This channel has the lowest energy barrier ($\Delta E_0^{\ddagger}$ = 3.2 kcal/mol) and it is endothermic path ($\Delta E_0^{\ddagger}$ = 0.9 kcal/mol) at CBS-QB3//BMK/6-31+G(d,p). Compared to endothermic routes C_μ of 1.9 kcal/mol and C_β of 3.9 kcal/mol. An inspection of Table 1 indicates that the barrier heights are method dependent as reported by Moc and Simmie [57].

Table 1: Energy barriers ($\Delta E^{\#}_0$, kcal/mol) for H-abstraction from **MP** by $^{\bullet}$OH at different levels over temperature range 200–300 K at BMK/6-311++G(2d,2p)[a], BB1K/6311++G(2d,2p)[a], MP2/6-311++G(2d,2p)[a] and CBS-QB3.

Site	BMK	BB1K	MP2	CBS-QB3
MP-α	1.97	3.03	19.87	3.2
MP- μ	0.79	2.13	21.26	4.0
MP-β	1.02	2.36	22.07	4.3

[a]://BMK/6-31+G(d,p) geometry

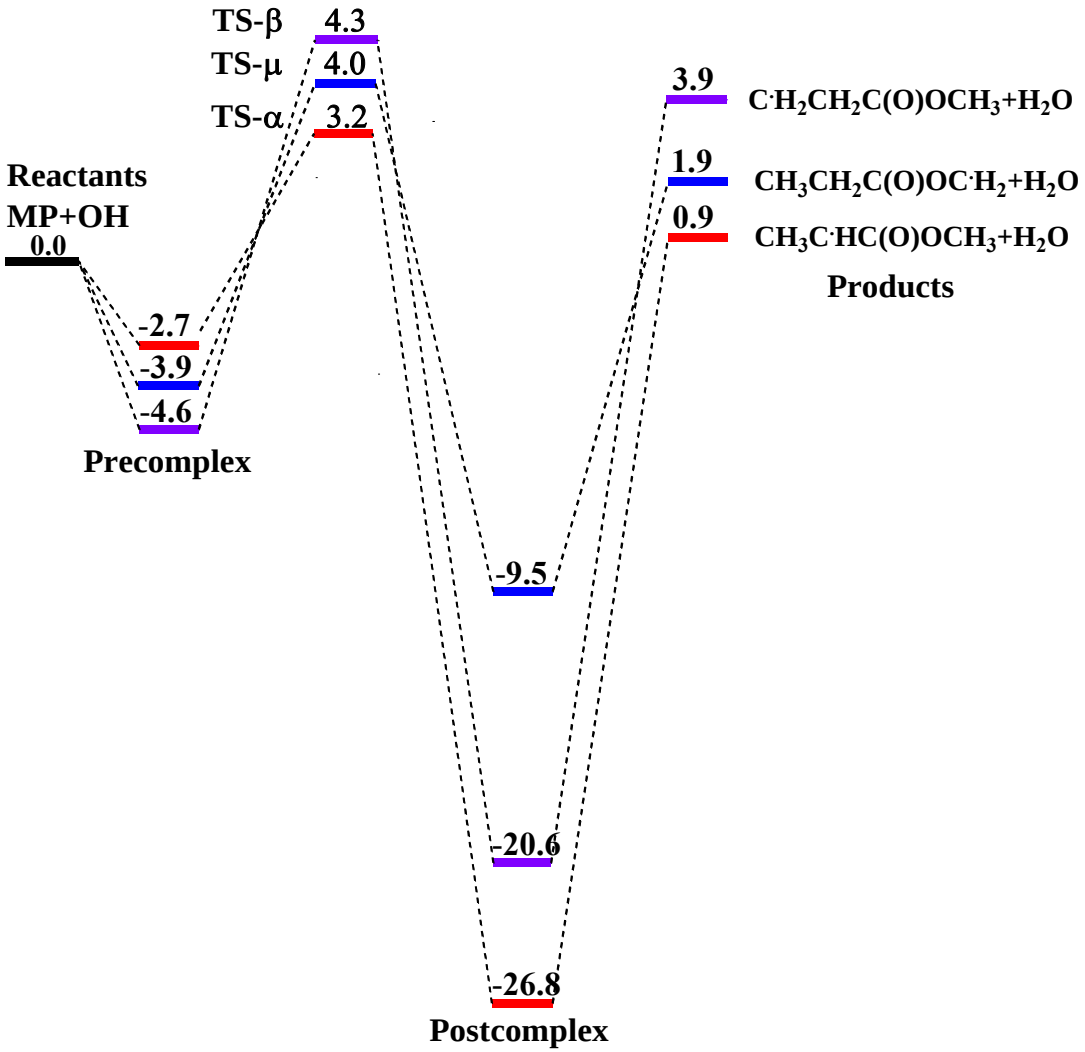

Fig. 3. Potential energy profile for bimolecular reaction of **MP** with ˙OH (ΔE_0, $\Delta E_0^{\ddagger}$, kcal/mol) using CBS-QB3.

3.3. Equilibrium constants

Equilibrium constants (K_{eq}) for all reactions (R1-R3) of **MP** were calculated over a temperature range from 200-300 K at 1 atm. Single point energy calculations for all stationary points were carried out at CBSQB3 level of theory. The computed K_{eq} values are depicted in Figs. 4, 5 and summarized in supporting information.

The branching ratio (Γ %) is the ratio between the individual rates and the total rate. Γ is an important value because it determines reaction pathways and products distribution. K_{eq} and the branching ratios (Γ) are summarized in supporting information. An inspection of Figs. 4, 5 indicates that hydrogen-abstraction from C_α

as the most preferable path over the whole investigated temperature range, followed by C_{μ} and a modest contribution from C_{β}. The order of K_{eq} correlates with the values of the energy barriers.

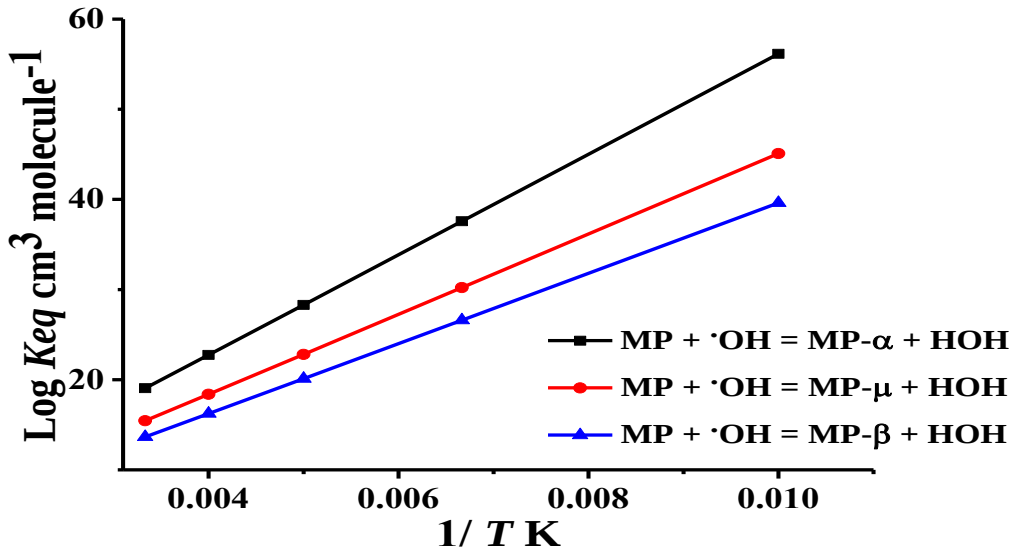

Fig. 4. Comparison of changes of K_{eq} for R1-R3 of **MP** oxidation with OH (at 200–300 K, 1 atm) at the CBS-QB3 level of theory.

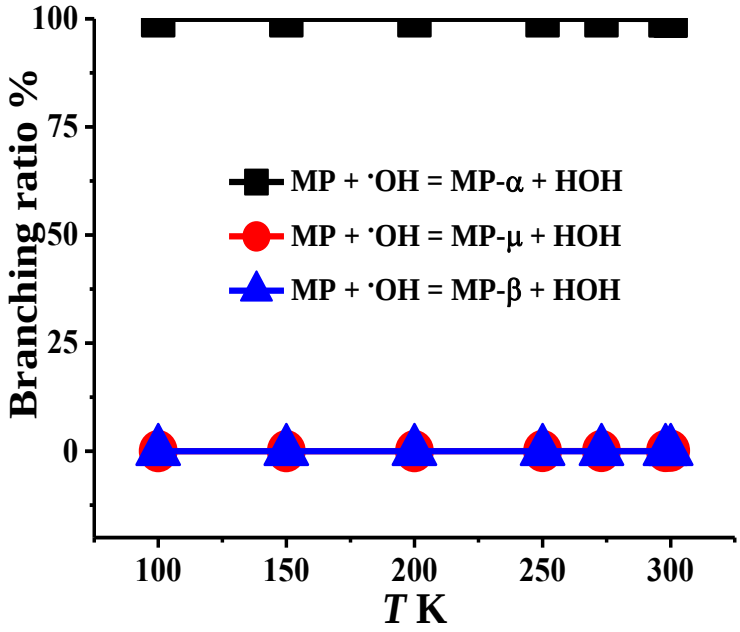

Fig. 5. Branching ratios (Γ) of each channel in the reaction of **MP** with ·OH at CBS-QB3 obtained by means of K_{eq}.

3. 4. Reaction rate constants

Rate constants ($k_{1\text{-}3}$) for all reactions are shown in Figs. 6 and 7. They were calculated using conventional transition state theory (TST) over an atmospheric temperature range from 200-300 K at 1 atm. Since an H-atom is involved in these reactions tunneling has to be considered. It was included by incorporating the Wigner (W) tunneling correction in the rate equation.

$k_{1\text{-}3}$ and the branching ratios (Γ) are summarized in Tables 2-4. An inspection of these Tables indicates the hydrogen-abstraction from C_α as a most preferable path over the whole investigated temperature range, followed by C_β and a modest contribution from C_μ. The order of $k_{1\text{-}3}$ does not parallel the values of the energy barriers. The frequency factors seem to be the main player in determining priority of different channels [22]. Plotting of log k against $1/T$ K shows an Arrhenius behavior over the considered temperatures range and the rate equation can be well described by the normal Arrhenius parameters equation ($k = A\ \exp(-E_a/RT)$).

The total rate ($k_{1\text{-}3}$) is the sum of the individual rate constants estimated at 200-300 K and 1 atm, and they are given in Table 2. We observe that the quantum tunneling effects vary, tunneling is 2 times greater for H-abstraction from the $-CH_3$ group than from the $-CH_2$ group. The total rate constant for OH oxidation is estimated to be 5.96×10^{-12} cm^3 molecule^{-1} s^{-1} at 298 K. The corresponding rate coefficients are summarized in Table 2. Le Calve et al [13]. utilized the pulsed laser photolysis-laser induced fluorescence technique over the temperature range of 253 to 372 K and derived the Arrhenius expression of $(8.73 \pm 2.53) \times 10^{-12}$ exp(-(148 ± 86)/T) cm^3 molecule^{-1} s^{-1}. Andersen et al [10]. measured the rate constant at 293 K with relative rate techniques as 9.25×10^{-13} cm^3 molecule^{-1} s^{-1} and also theoretically obtained the rate coefficient of 3.8×10^{-13} cm^3 molecule^{-1} s^{-1} at 298 K, with TST and energies at the CCSD(T)/cc-pVTZ//BH&HLYP/aug-cc-pVTZ level. Compared to these experimental rate coefficients, our predictions are in excellently agreement with Le Calve et al.'s results [13], Andersen et al [10]. and Cavalli et al [11].

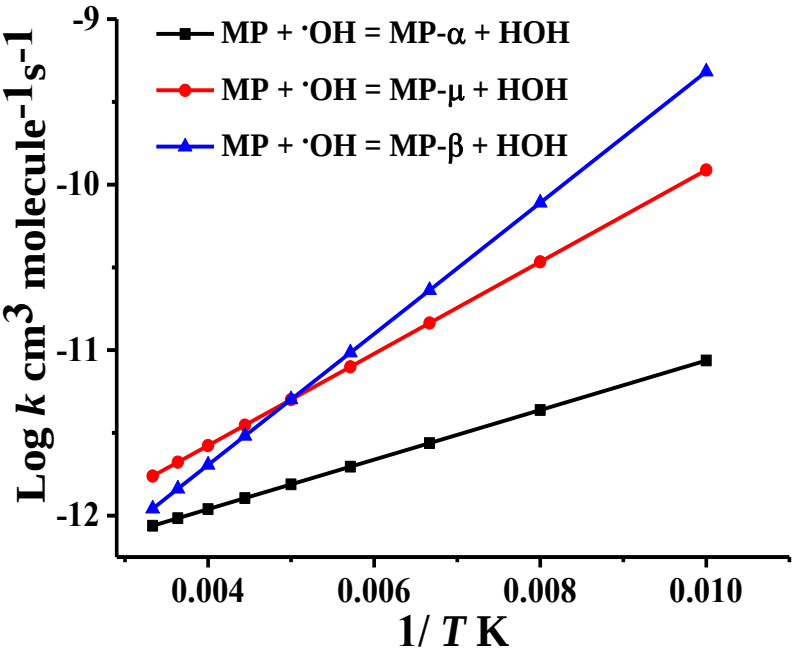

Fig. 6. Bimolecular rate constants $k_{1\text{-}3}$ for reaction channels of **MP** oxidation with ·OH obtained by means of TST/W theory (T = 200–300 K, P = 1 atm) according to the computed CBS-QB3 energies.

Table 2. Rate constants ($k_{1\text{-}3}$, cm^3 molecule^{-1} s^{-1}) for **MP** oxidation with ·OH from TST and TST/W calculations (T = 200–300 K, P = 1 atm) based on CBS-QB3 energies.

	R1, k_1			R2, k_2			R3, k_3			k_{Total}
T K	TST	TST/W	$\chi(T)$	TST	TST/W	$\chi(T)$	TST	TST/W	$\chi(T)$	$k_{1\text{-}3}$
200	1.07E-13	8.11E-12	1.98	8.13E-12	2.99E-12	3.35	8.67E-12	2.98E-12	3.82	3.10E-11
250	1.75E-13	9.61E-12	1.63	9.80E-12	5.76E-12	2.50	1.48E-13	6.94E-12	2.80	3.24E-11
273	6.77E-13	1.03E-12	1.53	9.53E-13	2.15E-12	2.26	5.90E-13	1.48E-12	2.51	6.88E-12
298	6.78E-13	9.79E-13	1.44	8.76E-13	1.80E-12	2.06	4.99E-13	1.13E-12	2.27	5.96E-12

Table 3. Two-parameters Arrhenius[a] coefficients for oxidation of **MP** by ·OH from TST/W calculations (T = 200-300 K, P = 1 atm) using CBS-QB3 energies.

Parameter/channel	C_α	C_β	C_μ
A	2.75E-13	5.28E-14	2.06E-13
E_a	-0.69	-1.81	-1.27

[a] $k = A \exp(-E_a/RT)$: The units of *k*, *A* are cm^3 $molecule^{-1}$ s^{-1} and E_a in kcal/mol.

3. 4. 1. Branching ratios

The branching ratios of rate constants for all reactions are shown in Fig. 7. Table 4 collects the percentage contribution of each channel. The hydrogen-abstraction from C_α and C_β was found to be the dominant paths. Abstraction from C_α shows the largest contribution at low temperature up to 200 K but decreases at higher temperature to 44.1 % from the total rate at 300 K. Rising of temperature (above 200 K) increases significantly the rate of hydrogen atom abstraction from C_μ. The order of rate constants was not found to be in agreement with the values of the energy barriers whereas K_{eq} does. The frequency factors seem to be the main player in determining priority of different channels [22]. Our calculated rate constants and branching ratios help to illuminate combustion properties of **MP**. This analysis shows that knowledge of accurate rate constants and branching ratios is crucial to accurately elucidate combustion properties of different fuels. Therefore, a thorough investigation of the bimolecular reaction kinetics of **MP** is required to improve the accuracy of combustion models and also to describe the combustion behavior of biodiesel fuels.

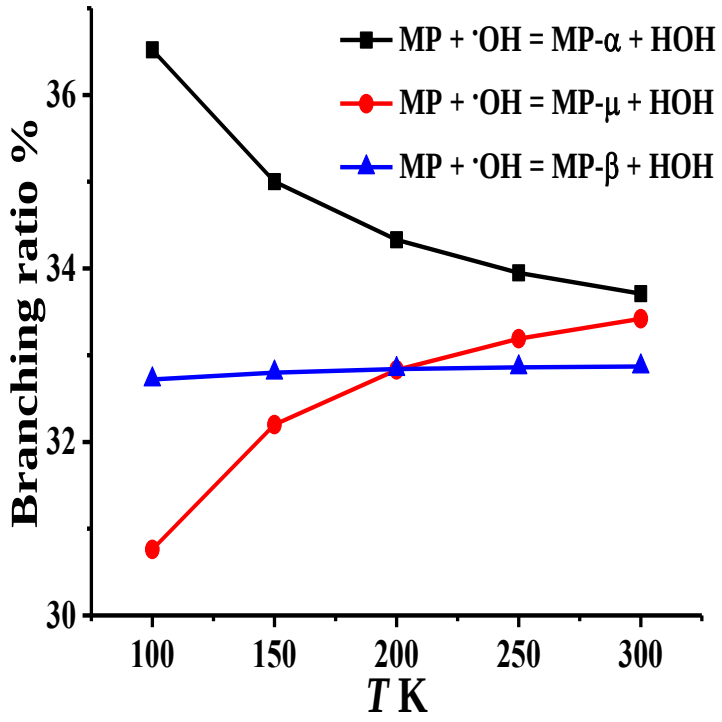

Fig. 7. Branching ratios (*Γ*) in the reaction of **MP** with ·OH at CBS-QB3 by means of TST/W.

Table 4. Branching ratio (*Γ*) of each channel in the reaction of **MP** with ·OH at CBS-QB3 obtained by means of TST/W.

T K	*Γ*-*α*	*Γ*-*μ*	*Γ*-*β*
200	34.33	32.83	32.84
250	33.95	33.19	32.86
273	33.18	33.31	33.51
298	36.80	31.51	31.70

4. Conclusion

This paper describes thermochemistry and kinetics of the reaction of **MP** with ·OH at BMK, BB1K, MP2, and CBS–QB3 levels of theories. The results obtained can be summarized as follows:

1. Based on the calculated energy barriers, the order of H-abstraction reactions from **MP** by the OH radical was found to be $\alpha < \mu < \beta$ at CBS–QB3//BMK/6-31+G(d,p).

2. The branching ratios show H-abstraction from the C_α and C_β positions as a most dominant reaction.

3. Formation of water from C_β is an exothermic reaction, while the other two routes are endothermic.

4. Preferable H-abstraction from C_α–H was attributed to the weakness of C–H bond, while the feasibility of abstraction from C_β was explained in term of hydrogen bond stabilization of transition state.

Appendix A. Supplementary material

Supplementary data associated with this article can be found, in the online version, at

References

1. Dievart, P., Won, S. H., Dooley, S., Dryer, F. L., Ju, Y., *"A kinetic model for methyl decanoate combustion", Combust. Flame J.*, 2012, 159, 1793−1805.
2. Herbinet, O., Pitz, W. J., Westbrook, C. K., *"Detailed chemical kinetic oxidation mechanism for a biodiesel surrogate", Combust. Flame J.*, 2008, 154, 507–528.
3. Westbrook, C. K., Naik, C. V., Herbinet, O., Pitz, W. J., Mehl, M., Sarathy, S. M., *"Detailed chemical kinetic reaction mechanisms for soy and rapeseed biodiesel fuels", Combust. Flame J.*, 2011, 158, 742–755.
4. Herbinet, O., Pitz, W. J., Westbrook, C. K., *"Detailed chemical kinetic mechanism for the oxidation of biodiesel fuels blend surrogate", Combust. Flame J.*, 2010, 157, 893–908.
5. Dievart, P., Won, S. H., Gong, J., Dooley, S., Ju, Y., *"A comparative study of the chemical kinetic characteristics of small methyl esters in diffusion flame extinction", Proc. Combust. Inst. J.*, 2013, 34, 821−829.
6. Ifang, S., Benter, T., Barnes, I., *"Reactions of Cl atoms with alkyl esters: kinetic, mechanism and atmospheric implications", Environ Sci Pollut Res. J.*, 2015, 22, 4820–4832.
7. Koppmann, R., *"Volatile organic compounds in the atmosphere"*, New York: Wiley-Blackwell, 2007, 129–130.

8. Chan, T. C. E., Marcello, M., Psaro, R., Ravasio, N., Zaccheria, F., *"New generat in biofuels: c-valerolactone into valeric esters in one pot", RSC Adv. J.*, 2013, 3, 1302–1306.
9. Andersen, V. F., Ørnsø, K. B., Jørgensen, S., Nielsen, O. J., Johnson, M. S. *"Atmospheric chemistry of ethyl propionate", Phys. Chem. A J.*, 2012, 116, 5164-5179.
10. Andersen, V. F., Bernhanu, T. A., Nilsson, E. J., Jørgensen, S., Nielsen, O. J., Wallington, T. J., Johnson, M. S., *"Atmospheric chemistry of two biodiesel model compounds: methyl propionate and ethyl acetate", Phys. Chem. A J.*, 2011, 115, 8906.
11. Cavalli, F., Barnes, I., Becker, K. H., *"Atmospheric oxidation mechanism of methyl propionate", Phys. Chem.* A *J.*, 2000, 104, 11310-11317.
12. Sun, X., Hu, Y., Xu, F., Zhang, Q., Wang, W., *"Mechanism and kinetic studies for OH radical-initiated atmospheric oxidation of methyl propionate", Atm. Environ. J.*, 2012, 63, 14-21.
13. Calve, S. L., Bras, G. L., Mellouki, A., *"Kinetic studies of OH reactions with a series of methyl esters", J. Phys. Chem. A* 1997, 101, 9137-9141.
14. Farooq, A., Davidson, D.F., Hanson, R.K., Westbrook, C.K., *"A comparative study of the chemical kinetics of methyl and ethyl propanoate", Fuel J.*, 2014, 134, 26–38.
15. Wang, Y. L., Lee, D. J., Westbrook, C. K., Egolfopoulos, F. N., Tsotsis, T. T., *"Oxidation of small alkyl esters in flames", Combust. Flame J.*, 2014, 161, 810−817.
16. Tan, T., Yang, X., Jub, Y., Carter, E. A., *"Ab initio kinetics studies of hydrogen atom Ab initio kinetics studies of hydrogen atom abstraction from methyl propanoate abstraction from methyl propanoate", Phys. Chem. Chem. Phys. J.*, 2016, 18, 4594-4607.
17. Tan, T., Pavone, M., Krisiloff, D. B., Carter, E. A., *"Ab initio reaction kinetics of hydrogen abstraction from methyl formate by hydrogen, methyl, oxygen, hydroxyl, and hydroperoxy radicals", Phys. Chem. A J.*, 2012, 116, 8431–8443.
18. Tan, T., Yang, X., Krauter, C. M., Ju, Y., Carter, E. A., *"Ab initio kinetics of hydrogen abstraction from methyl acetate by hydrogen, methyl, oxygen, hydroxyl, and hydroperoxy radicals", Phys. Chem. A J.*, 2015, 119, 6377−6390.

19. Billaud, F., Dominguez, V., Broutin, P., Busson, C., *"Production of hydrocarbons by pyrolysis of methyl esters from rapeseed oil", Am. Oil. Chem. Soc. J.*, 1995, 72, 1149–1154.
20. El-Nahas, A.M., Mangood, A.H., Takeuchi, H., Taketsugu, T., *"Thermal decomposition of 2-butanol as a potential non fossil fuel: a computational study", Phys. Chem. A J.*, 2011, 115, 2837–2846.
21. El-Nahas, A.M., Mangood, A.H., El-Meleigy, A. B., *"A computational study on the structures and energetics of isobutanol pyrolysis", Comp. Theo. Chem. J.*, 2012, 997, 94–102.
22. El-Nahas, A.M., Mangood, El-Shereafy, E. E., El-Meleigy, A. B., *"Thermo-chemistry and kinetics of isobutanol oxidation by the OH radical", Fuel J.*, 2013, 106, 431–436.
23. El-Nahas, A.M., Uchimaru, T., Sugie, M., Tokuhashi, K., Sekiya, A., *"Hydrogen abstraction from dimethyl ether DME and dimethyl sulfide DMS by OH radical: a computational study", Mol. Struct. Theo. Chem. J.*, 2005, 722, 9–19.
24. El-Nahas, A.M., Bozzelli, J.W., Simmie, J.M., Navarro, M.V., Black, G., Curran, H.J., *"Thermochemistry of acetonyl and related radicals", Phys. Chem. A J.*, 2006, 110, 13618–13623.
25. El-Nahas, A.M., Navarro, M.V., Simmie, J.M., Bozzelli, J.W., Curran, H.J., Dooley, S., Metcalfe, W., *"Enthalpies of formation, bond dissociation energies and reaction paths for the decomposition of model biofuels: ethyl propanoate and methyl butanoate", Phys. Chem. A J.*, 2007, 111, 3727–3739.
26. El-Nahas, A. M., Simmie, J. M., Navarro, M. V., Bozzelli, J. W., Black, G., Curran H. J., *"Thermochemistry and kinetics of acetonyl peroxy radical isomerisation and decomposition: a quantum chemistry and CVT/SCT approach", Phys. Chem. Chem. Phys. J.*, 2008, 10, 7139–7149.
27. El-Nahas, A.M., Heikal, L.A., Mangood, A.H., El-Shereefy, E.-S., *"Structures and energetics of unimolecular thermal degradation of isopropyl butanoate as a model biofuel: density functional theory and ab initio studies", Phys. Chem. A J.*, 2010, 114, 7996–8002.
28. Mahmoud, Mohamed A. M., El-Demerdash, S. H., Mangood, A. H., El-Nahas, A. M., *"Modeling of thermochemistry of thermal decomposition of methyl propionate and ethyl acetate biodiesel", IJASTR. J.*, 2017, 7, 2, 190-202.

29. Boese, A. D., Martin, J. M. L., *"Development of density functionals for thermochemical kinetics", Chem. Phys. J.*, 2004, 121, 3405–3416.
30. Merrick, J. P., Moran, D., Radom, L., *"An evaluation of harmonic vibrational frequency scale factors", Phys. Chem. A J.*, 2007, 111, 11683-11700.
31. Gonzalez, C., Schlegel, H. B., *"An improved algorithm for reaction path following", Chem. Phys. J.*, 1989, 90, 2154-2161.
32. Gonzales, C., Schlegel, H. B., *"Reaction path following in mass-weighted internal coordinates", Phys. Chem. J.*, 1990, 94, 5507–5523.
33. Fukui, K., *"The path of chemical reactions e the IRC approach", Acc. Chem. Res. J.*, 1981, 14, 363-368.
34. Becke, A. D., *"Density-functional thermochemistry. IV. A new dynamical correlation functional and implications for exact-exchange mixing", Phys. Chem. J.*, 1996, 104, 1006–1040.
35. Zhao, Y., Lynch, B. J., Truhlar, D. G., *"Development and assessment of a new hybrid density functional model for thermochemical kinetics", Phys. Chem. A J.*, 2004, 108, 2709–2715.
36. Møller, C., Plesset, M. S., *"Note on an approximation treatment for many electron systems", Phys. Rev. J.*, 1934, 46, 618-622.
37. Ochterski, J. W., Petersson, G. A., Montgomery, J. A., *"A complete basis set model chemistry. V. Extensions to six or more heavy atoms", J. Chem. Phys.* 1996, 104, 2598-2619.
38. Montgomery, Jr. J. A., Frisch, M. J., Ochterski, J. W., Petersson, G. A., *"A complete basis set model chemistry: VI. Use of density functional geometries and frequencies", Chem. Phys. J.*, 1999, 110, 2822–2827.
39. Montgomery, Jr. J. A., Frisch, M. J., Ochterski, J. W, Petersson, G. A., *"A complete basis set model chemistry. VII. Use of the minimum population localization method", Chem. Phys. J.*, 1999, 110, 2822–2827.
40. Montgomery, Jr. J. A., Frisch, M. J., Ochterski, J. W., Petersson, G. A., *"A complete basis set model chemistry. VII. Use of the minimum population localization method", Chem. Phys. J.*, 2000, 112, 6532–6542.
41. Pokon, E. K., Liptak, M. D., Feldgus, S., Shields, G. C., *"Comparison of CBS–QB3, CBS–APNO, and G3 predictions of gas phase deprotonation data", Phys. Chem. A J.*, 2001, 105, 10407–10483.

42. Frisch, M.J., Trucks, G.W., Schlegel, H.B., Scuseria, G.E., Robb, M.A., Cheeseman, J.R., Scalmani, G., Barone, V., Mennucci, B., Petersson, G.A., Nakatsuji, H., Caricato, M., Li, X., Hratchian, H.P., Izmaylov, A.F., Bloino, J., Zheng, G., Sonnenberg, J.L., Hada, M., Ehara, M., Toyota, K., Fukuda, R., Hasegawa, J., Ishida, M., Nakajima, T., Honda, Y., Kitao, O., Nakai, H., Vreven, T., Montgomery Jr, J.A., Peralta, J.E., Ogliaro, F., Bearpark, M., Heyd, J.J., Brothers, E., Kudin, K.N.,Staroverov, V.N., Kobayashi, R., Normand, J., Raghavachari, K., Rendell, A.,Burant, J.C., Iyengar, S.S., Tomasi, J., Cossi, M., Rega, N., Millam, J.M., Klene, M., Knox, J.E., Cross, J.B., Bakken, V., Adamo, C., Jaramillo, J., Gomperts, R., Stratmann, R.E., Yazyev, O., Austin, A.J., Cammi, R., Pomelli, C., Ochterski, J.W., Martin, R.L., Morokuma, K., Zakrzewski, Voth, V.G., Salvador, G.A., Dannenberg, P., Dapprich, J.J., Daniels, S., Farkas, A.D., Foresman, O., Ortiz, J.B., Cioslowski, J.V., Fox, J., Gaussian 16 Revision A.03, Gaussian, Inc.: Wallingford, CT, 2016.
43. Zhurko, G. A. Chemcraft V1.8. http://www.Chemcraftprog.com.
44. Steinfeld, J. I., Francisco, J. S., Hase, W. L., *"Chemical kinetics and dynamics. Upper saddle river"*, Prentice-Hall, NJ 1999.
45. Johnston, H.S., *"Gas-Phase Reaction Rate Theory"*, New York: The Ronald Press, 1966.
46. Truhlar, D. G., Garrett, B. C., Klippenstein, S. J., *"Current status of transition state theory", Phys. Chem. J.*, 1996, 100, 12771–12800.
47. Steinfeld, J. I., Francisco J. S., Hase, W. L., *"Chemical kinetics and dynamics"*, Prentice-Hall, Englewood Cliffs, NJ 1989.
48. Lendvay, G., *"Bond orders from ab initio calculations and a test of the principle of bond order conservation", Phys. Chem. J.*, 1989, 93, 4422–4429.
49. Reed, A. E., Curtiss, L. A., Weinhold, F., *"Intermolecular interactions from a natural bond orbital, donor-acceptor viewpoint", Chem. Rev. J.*, 1988, 88, 899-926.
50. Rapp, D., *"Statistic Mechanics"*, New York: Holt, Rinehart & Winston, 1972.
51. Truhlar, D.G., Isaacson, A.D., Garrett, B.C., *"Generalized Transition State Theory, Theory of Chemical Reaction Dynamics"*, vol. 4, CRC Press, Boca Raton, FL, 1985. p. 65 (Chapter 2).
52. Gilbert,R. G., Smith, S.C., *"Theory of unimolecular and recombination*

reactions", Black well Scientific, Oxford 1990.

53. Rao, H., Zeng, X., He, H., Li, Z. R., *"Theoretical investigations on removal reactions of ethanol by H atom", Phys. Chem. A J.*, 2011, 115, 1602-1608.
54. Canneaux, S., Bohr, F., Henon, E., *"KiSThelP: a program to predict thermodynamic properties and rate constants from quantum chemistry results", Comput. Chem. J.*, 2014, 35, 82–93.
55. Huber, K. P., Herzberg, G., *"Molecular spectra and molecular structure. IV. Constants of diatomic molecules",* New York: Van Nostrand Reinhold, 1979.
56. Hammond, G. S., *"A correlation of reaction rates", Am. Chem. Soc. J.*, 1955, 77, 334-338.
57. Moc, J., Simmie, J.M., *"Hydrogen abstraction from n-butanol by the hydroxyl radical: high level ab initio study of the relative significance of various abstraction channels and the role of weakly bound intermediates", Phys. Chem. A J.*, 2010, 114, 5558-5564.